MADRID
inter.noise 2019
June 16 - 19
NOISE CONTROL FOR A BETTER ENVIRONMENT

A new approach for real-time sound insulation filters development

Muhammad, Imran[1]
Heimes, Anne
Vorländer, Michael
Institute of Technical Acoustics
RWTH Aachen University, Germany

ABSTRACT

Auralization of sound insulation has become a valuable tool to assess the perceptual aspects of sound transmission in built environments. One advanced goal is to appropriately describe the influence of noise disturbance on human cognitive performance in the built environment. Methods for auralization of sound insulation are available with several simplifications that are implicit in the formulation of ISO 12354. There, the transfer functions from source to receiver room are only valid for diffuse-field assumptions, i.e. for arbitrary point to point transmission. One further simplification is that the sound is apparently radiated from one point representing the whole bending wave pattern on the wall. In this paper, we introduce a new technique for computing sound insulation filters for virtual acoustic scenes in buildings with respect to more complex sound propagation effects. At first, we consider the source room reverberation and the source directivity. Secondly, the transfer functions from source to receiver rooms are calculated for extended walls by using a distribution of secondary sound sources. The receiving room acoustics is implemented in a way that it encompasses the reverberation based on room geometry, absorption and binaural transfer functions between the radiating walls and the receiver.

Keywords: Airborne Sound Insulation, Building Acoustics, Auralization, Virtual Reality
I-INCE Classification of Subject Number: 30

1. INTRODUCTION

In this paper, we present an extended approach to construct filters for binaural sound transmission between rooms separated by building elements. This approach is based on ISO 12354 for airborne sound transmission in order to build up an auralization tool for psychoacoustic sound insulation assessment. We take into consideration the spatial variation of the sound field inside the rooms that enables us to experience binaural sound from arbitrarily positioned sound sources inside the source room. Moreover, we consider the synthesis of the room impulse response (RIR) from one-third octave band values of the reverberation time based on ISO standards. In this way, the proposed approach increases interaction with virtual environments, making a more realistic and immersive scene and leads toward an accurate subjective evaluations of building performance.

[1] email: mim@akustik.rwth-aachen.de

Several simplifications exist in our previously developed building acoustic auralization framework [1-3] and in the formulation of ISO 12354 on which it is based on. At first, it is assumed that the incident sound intensity on the building elements is equal for all transmission paths. In other words, the same incident sound intensity impinges all elements independent of the source position, its directivity and room geometries. Secondly, the transfer functions calculated from source room to receiver room are only valid for point to point transmission [4], however, extended walls are always present in real situations. In the receiving room, the simplification is made that the sound is apparently radiated from one point representing the whole (bending) wave pattern on the wall [5].

In our new approach, the focus is on addressing these challenges for more accurate filter construction and representation of physically correct building acoustics auralization. To achieve this, in first place, we take into consideration the source room reverberation depending on the room characteristics and the sound source directivity. Secondly, the transfer functions from source to receiver rooms are calculated for extended walls by using concept of dividing the individual building element into a multitude of secondary sound sources with non-uniform energy distribution. Thirdly, the receiver room acoustics is implemented in a way that it includes the receiving room reverberation based on room geometry, absorption and binaural transfer functions between radiating walls and the receiver.

2. ESTABLISHED METHODS

In building acoustics, the first application of auralization of airborne sound insulation was introduced by Vorländer and Thaden [6]. Based on the prediction method ISO 12354, they developed a framework that made it possible to auralize the sound insulation through binaural technology. Later, Vorländer and Imran [5, 6] implemented real-time insulation auralization and extended it as a Virtual Reality application for subjective evaluation of sound insulation in built environments. As a result, extended work by Imran et al. [4] is implemented in the sound insulation software, developed in Unity 3D environment for integration of audio cues into virtual reality environments. Some improvements have been made to the sound insulation calculation for the reverberant sound field to include the synthesized RIR based on one-third octave band values of the reverberation time computed from ISO standards [7].

The standardised sound level difference, D_{nT}, expressed by the transmission coefficients $\tau_{ij} = 10^{-0.1R_{ij}}$ of all transmission paths between two rooms is given in [7] (Equation 1). Here, V is the volume of the receiving room and S_D the area of the separating (direct) element.

$$D_{nT} = -10\log\sum_{\forall ij}\tau_{ij} + 10\log\frac{0.32V}{S_D} \tag{1}$$

The average sound pressure level in the receiver room is given by Equation 2, and in its energy formulation in Equation 3. Here, p_R^2 and p_S^2 are mean squared pressures in the receiving and source room, respectively.

$$L_R = L_S + 10\log\sum_{\forall ij}\tau_{ij} + 10\log\left(\frac{S_D}{0.32V}\frac{T}{0.5}\right) \tag{2}$$

$$p_R^2 = p_S^2\frac{S_D}{0.32V}\frac{T}{0.5}\sum_{\forall ij}\tau_{ij} \tag{3}$$

The radiating elements are approximated as point sources on the walls, and the balance between direct and reverberant sound field is computed through the ratio of energies given by $\frac{E_{rev}}{E_{dir}} = \frac{16\pi r^2}{A}$, with E_{dir} and E_{rev} as the energies of direct and reverberant sound field at a distance r from the sound source [5]. A is the equivalent absorption area of the receiving room. For uncorrelated direct and reverberant sound fields, the contribution of the transmission path ij to the mean squared pressure in terms of the reverberant and the direct field can be written as $p_{R,ij}^2 = p_{R,ij,dir}^2 + p_{R,ij,rev}^2$.

In order to introduce the reverberation of the receiving room, its impulse response, $h(t)$, is simulated or measured. At first, the direct sound is removed from that impulse response as it is already included in the transmission path calculation in its binaural form $\boldsymbol{HRIR}\left(\mathrm{t} - \frac{r_j}{c}, \theta_j, \varphi_j\right)$. Subsequently, it is approximately equalised to white spectrum and normalised in energy. The time domain representation of the binaural signal from source to receiver of the transmission path ij is given in Equation 4.

$$p_{R,ij}(t) = \sqrt{\frac{S_D}{0.32V}\,\frac{T}{0.5}\,\frac{\tau_{ij}}{16\pi r_{ij}^2 + A}}\;\boldsymbol{p_s}(\boldsymbol{t}) * \left[\sqrt{A}\,\boldsymbol{HRIR}\left(\mathrm{t} - \frac{r_j}{c}, \theta_j, \varphi_j\right) + \sqrt{16\pi r_{ij}^2}\,\boldsymbol{h}(\boldsymbol{t})\right] \qquad (4)$$

All binaural contributions from the radiating elements are summed up to get final signal.

3. IMPROVED METHOD

This section describes a new approach for sound insulation filter construction, still based on ISO 12354 [7] and our previous work [3-5]. But now, simplifications are addressed which exist in our previously developed real-time building acoustic auralization framework [4]. In this new approach, the incident sound field varies for all transmission paths depending on the sound pressure hitting the corresponding building elements, due to source position and source directivity. Secondly, the influence of the reverberation and the balance between direct and reverberant energies inside the source room and receiving room are considered for the transfer function construction process. These transfer functions are developed for extended radiating walls treated as multiple point sources (secondary sources) rather than considering these walls as single point sources in the receiving room.

The direct sound field can be assumed to propagate as in free-field conditions, whilst the reverberant field is uniformly distributed in the rooms [8, 9]. This phenomenon is shown through the classical sound field theory for sound propagation in rooms from Equation 5.

$$L_S = L_W + 10\log\left(\frac{Q_S}{4\pi r^2} + \frac{4}{A_S}\right) \qquad (5)$$

Equation 5 inherently incorporates the influence of the room reverberation, the directivity of the source, and the same balance between direct and reverberant energy as considered in approach [4]. Here, L_S is the sound pressure level, L_W is the sound power level, Q_S is source directivity normalised to 1 for the omnidirectional case, and A_S is equivalent absorption area of the source room. The mean squared sound pressure at a point inside the source room in energetic notations is given by Equation 6, with $P_a = 10^{-12}10^{-0.1L_W}$ (source acoustic power in Watts).

$$p_S^2 = \rho c\, P_a \left(\frac{Q_S}{4\pi r^2} + \frac{4}{A_S}\right) \tag{6}$$

The typical source and receiver rooms are shown in the Figure 1. Here, the sound source (example: vibrating back-baffled piston) is selected to analyse the influence of the directivity of the source, i.e. the different incident sound power impinges different elements, depending on the source directivity and position.

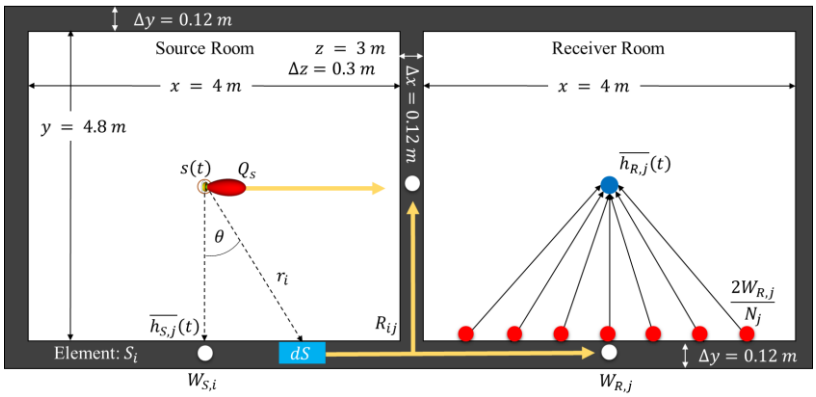

Figure 1: *Typical adjacent source and receiver rooms*

The incident sound power on any element i with an area S_i in the source room is a combination of the direct sound and the reverberant sound fields. Under diffuse sound field conditions, the reverberant part of the incident sound power, $W_{S,rev}$, is given by Equation 7.

$$W_{S,rev} = \frac{p_{S,rev}^2}{4\rho c} S_i = P_a \frac{S_i}{A_S} \tag{7}$$

Under free-field conditions, the direct incident sound power $W_{S,dir}$ is given in Equation 8.

$$W_{S,dir} = \frac{P_a}{4\pi} \int_S \frac{Q_S}{4\pi r^2} |\cos\theta| dS \tag{8}$$

r is the distance from the source to the surface element dS, θ is incidence angle from the source point to the element dS. Q_S, r and θ depend on the room geometries. Let the integral inside Equation 8 be represented by $F_i = \int_S \frac{Q_S}{4\pi r^2} |\cos\theta| dS$. By combining Equation 7 and Equation 8, the incident sound power on the element i can be calculated by using Equation 9.

$$W_{S,i} = P_a \left(\frac{F_i}{4\pi} + \frac{S_i}{A_S}\right) \tag{9}$$

The sound power transmitted from i^{th} element of the source room to j^{th} element of the receiver room for direct as well as flanking paths is defined by Equation 10, which is the final sound power of any radiating element j in the receiver room.

$$W_{R,ij} = \frac{P_a \cdot \tau_{ij} \cdot S_D}{S_i} \left(\frac{F_i}{4\pi} + \frac{S_i}{A_S}\right) \tag{10}$$

Therefore, the mean squared sound pressure for path ij in the receiving room can be computed by Equation 11.

$$p_{R,ij}^2 = \rho c \cdot W_{R,ij}\left(\frac{Q_j}{4\pi r_j^2} + \frac{4}{A_R}\right) \tag{11}$$

Q_j represents the directivity of the radiating element j of the receiving room with an equivalent absorption area A_R, and r_j represents the distance between the acoustic centre of the radiating element j to the evaluation point (position of the receiver).

4. FILTER CONSTRUCTION

4.1 Sound source directivity

The source directivity Q_S in this example is computed by the formula of a cardioid source. The directivity is normalised to guarantee that $\int_S Q_S(\theta, \varphi) = 4\pi$ for $\theta = [0, \pi]$ and $\varphi = [0, 2\pi]$.

4.2 Room impulse response synthesis

We have adopted a procedure to synthesize $h(t)$ from the reverberation time, T, to include the effects of absorption of room boundaries as well as to simulate an equivalent real room. The approximated $h(t)$ is obtained through a linear combination of filtered exponential decay signals. Consider the signal, $g(t, T)$ as given in Equation 12, with $n(t)$ as a normally distributed random variable having zero mean and unit standard deviation. The signal $g(t, T)$ decays 60 dB for each T seconds for all frequency bands.

$$g(t, T) = \sqrt{\frac{2\ ln10^3}{T}} \cdot e^{-ln10^3 \frac{t}{T}} \cdot n(t) \tag{12}$$

The factor $\sqrt{\frac{2\ ln10^3}{T}}$ in Equation 12 normalizes $g(t, T)$ in energy. From the linear combinations of filtered signals, $g(t, T)$, the impulse response $h(t)$ is synthesized, which then decays at different rates for each frequency band (Equation 13).

$$h(t) = \sum_{\forall k} \alpha_k \cdot g(t, T_k) * F(t, k) \tag{13}$$

Here, T_k is reverberation time and the function $F_k(t, k)$ is a set of band-pass filters in time domain for each k^{th} one-third octave band. The function $g(t, T)$ tends to a white spectrum because of a convolution of the Fourier transform of $e^{-ln10^3 \frac{t}{T}}$ and a white spectrum of $n(t)$. However, there appear slight variations in the spectrum of $h(t)$ due to the statistical nature of $n(t)$, that must be compensated by α_k given in Equation 14.

$$\alpha_k = \frac{\sqrt{f_k\left(2^{\frac{1}{6}} - 2^{-\frac{1}{6}}\right)}}{\sqrt{\int_{-\infty}^{\infty}\left(g(t, T_k) * F_k(t, k)\right)^2 dt}} \tag{14}$$

4.3 Source room sound pressure level at boundaries

The synthesis of source room impulse responses to the surface elements is necessary to include the effects of absorption of room boundaries as well as to simulate the cases where an equivalent real room is not present (for outdoor sources). In the source room, the time-domain representation of the energetic form of Equation 6 is given in Equation 15, from which the sound pressure inside the source room at any point and on its walls is calculated. $s(t)$ is source signal normalized in power and $h_{S,i}(t)$ is energetically normalised impulse response of the source room [9].

$$p_S(t) = \sqrt{\rho c}\sqrt{P_a} \cdot s(t) * \left(\sqrt{\frac{Q_S}{4\pi r_i^2}} \cdot \delta\left(t - \frac{r_i}{c}\right) + \sqrt{\frac{4}{A_S}} \cdot h_{S,i}(t) \right) \tag{15}$$

As the integral inside Equation 8 is represented by F_i can be approximated numerically, for not very large elements and in not very close positions to the walls. This integral is obtained by assuming that Q_S, r and θ do not vary significantly along S_i, therefore these factors are taken out of the integral in Equation 16.

$$F_i \approx \frac{S_i Q_{S,i}}{4\pi R_i^2} |\cos\theta_i| \tag{16}$$

The vector R_i is the distance from the source to the centre of element i, with an incidence angle θ_i and $Q_{S,i}$ denotes mean directivity value for θ_i. In this method, the integral F_i is numerically calculated by the adaptive Simpson's integration method. The incident power on the element i, given in Equation 9, is represented by its corresponding instantaneous incident sound power in time domain in Equation 17.

$$W_{S,i}(t) = \sqrt{P_a} \cdot s(t) * \left(\sqrt{\frac{F_i}{4\pi}} \cdot \delta\left(t - \frac{r_i}{c}\right) + \sqrt{\frac{S_i}{A_S}} \cdot h_{S,i} \right) \tag{17}$$

4.4 Sound field in the receiving room

In [3, 4], the radiating elements in the receiving room are represented by single point sources. In the improved model, each radiating element j is represented by a set of evenly distributed point sources on its surface. The acoustic power of the radiating element j is distributed homogeneously among point sources by a factor $\frac{2}{N_j}$, [9]. After calculating $h_{R,j}(t)$ as an energetically normalized impulse response of the receiving room for a radiating element j, the contribution of the transmission path ij to the instantaneous sound pressure is computed by Equation 18.

$$p_{R,ij}(t) = \sqrt{\frac{P_a \tau_{ij} S_D \rho c_o}{S_i}} \cdot s(t) * \left(\begin{array}{c} \sqrt{\frac{Q_j \cdot F_i}{16\pi^2 r_j^2}} \cdot \boldsymbol{HRIR}(\boldsymbol{\theta_j}, \boldsymbol{\varphi_j}) + \sqrt{\frac{Q_j \cdot S_i}{4\pi r_j^2 A_S}} \cdot \boldsymbol{h_{S,i}}\left(\boldsymbol{t} - \frac{\boldsymbol{r_j}}{\boldsymbol{c}}\right) + \\ \sqrt{\frac{F_i}{\pi A_R}} \cdot \boldsymbol{h_{R,j}}\left(\boldsymbol{t} - \frac{\boldsymbol{r_i}}{\boldsymbol{c}}\right) + \sqrt{\frac{4S_i}{A_S A_R}} \cdot \left(\boldsymbol{h_{S,i}}(\boldsymbol{t}) * \boldsymbol{h_{R,j}}(\boldsymbol{t})\right) \end{array} \right) \tag{18}$$

Here, all $h(t)$ are statistically valid for all points inside both the source and the receiving rooms that is why $h(t)$ can be synthesized before implementing the

auralization filter chain. However, as it can be assumed that $h(t)$ does not vary significantly for different source/receiver positions, hence, $h_{R,j}(t)$ and $h_{S,i}(t)$ can be computed independently to avoid coherent interferences in the reverberant field coming from different radiating elements [6].

5. PERFORMANCE OF ALGORITHM

The real-time algorithmic processes for auralization are evaluated in terms of computational costs for each step involved. The processing time is calculated for main algorithm that are involved in real-time computations. All computations are performed on desktop personal computer featuring an Intel Core i7-7700 CPU @ 3.60 GHz multi-core with 16GB RAM, Windows 7 (64-bit) operating system.

Figure 2 shows plots for the latencies calculated for two main real-time processes. The first process includes computation of energies hitting at the surfaces of the each element i of source room that varies with the change in position and orientation of the source in real time and updating source room impulse responses for each element i. The second process involves the receiver room updates including receiver room impulse responses updating, handling of multiple secondary sources with HRTF updates due to receiver movements. In Figure 2a, the latencies of second process (real-time receiver room updates) are plotted. The computational cost increase exponentially with increase in the number of secondary on each element j. Figure 2b show the real-time computational cost for source room.

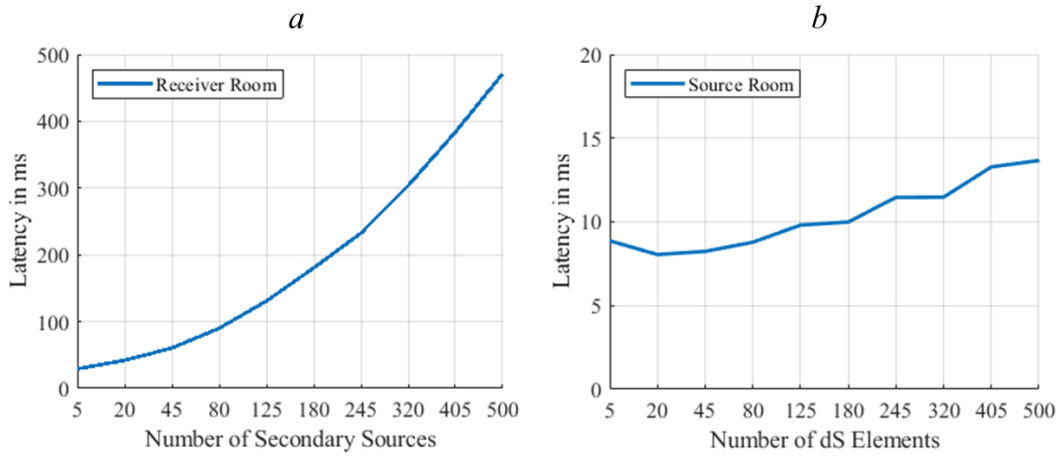

Figure 2: *Filter updated for a) secondary sources in the receiving room b) surface elements in the source room*

6. RESULTS

6.1 Visualization of direct irradiation

To visualize the sound pressure level in receiving room, it is selected a plane at 1.5 m above the floor inside the source and the receiver rooms for two positions and orientations of the sound source. First, the direct part of the final room impulse response is taken into account and the reverberation of the source as well as for the receiving rooms is excluded. Figure 3 and Figure 4 describe the spatial variation of the sound field inside the source room and the receiving room and provides a more detailed description of the sound transmission between the two rooms.

In Figure 3 the sound source is placed at the centre of the source room and

facing directly towards the separating element (main partition) of two rooms.

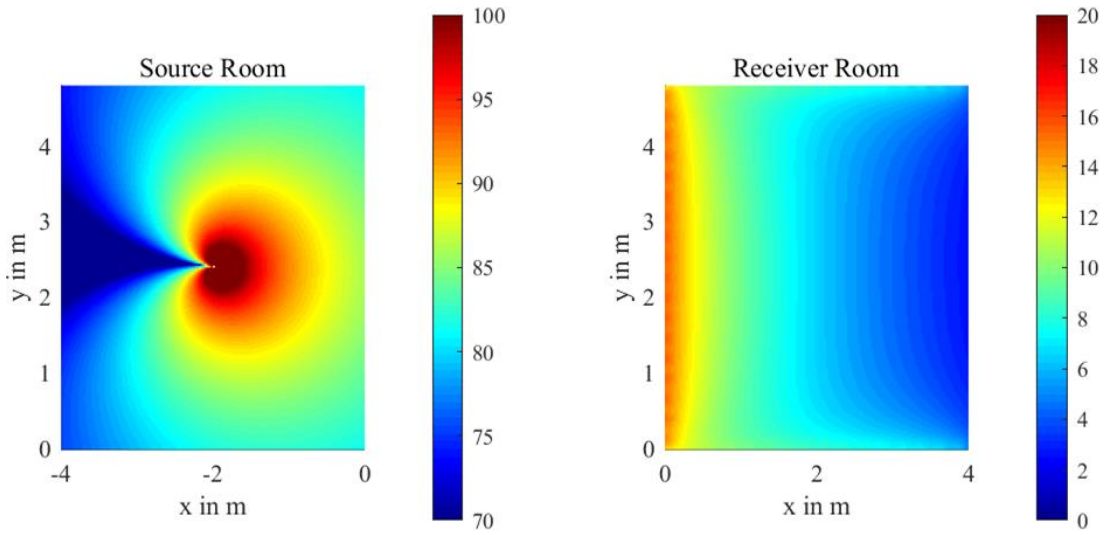

Figure 3: *Sound pressure level at* $z = 1.5m$ *height in source and receiving room for the direct part of sound field.*

In Figure 4, the sound source is placed near the left wall and facing towards it. The receiving room sound pressure level, SPL, for all paths clearly shows the effect of orientation and position of the source in receiver room. Here the contribution of the Dd path is small as compared to the contribution of Dd path in Figure 3. The difference between average SPL on the partition between both cases in 4.2dB.

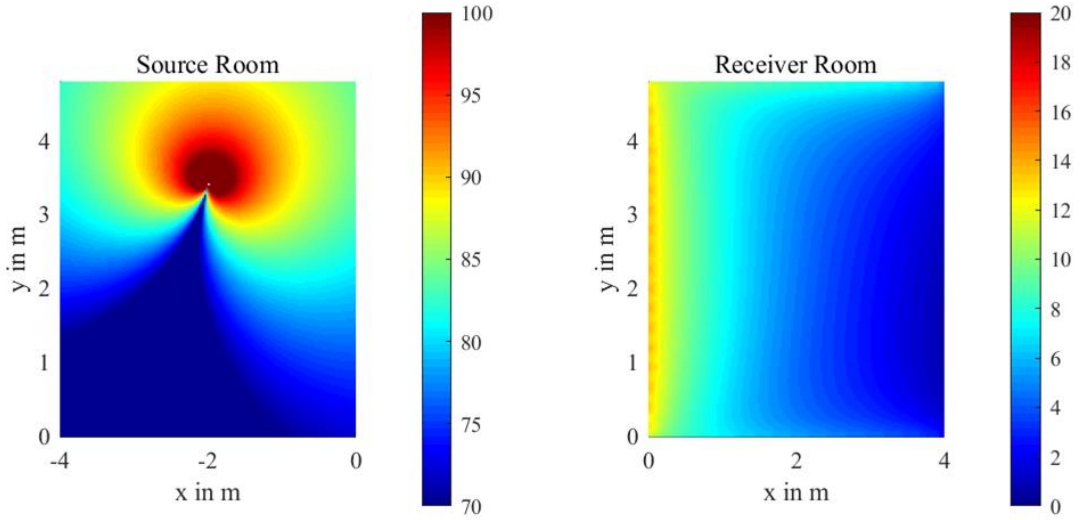

Figure 4: *Sound pressure level at* $z = 1.5$ m *height in source and receiving rooms for the direct part of sound field.*

6.2 Visualization of total SPL (direct and diffuse part)

Similarly, the reverberation of the source room and the receiving room are included in the sound pressure level calculations. The same procedure for visualization is applied for both source and receiving room as mentioned in the previous section.

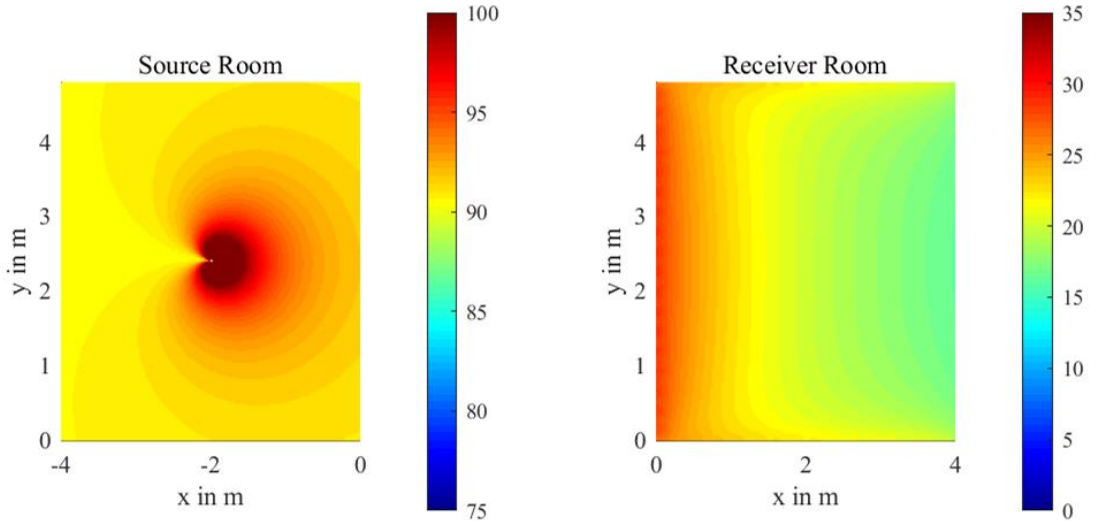

Figure 5: *Sound pressure level at* $z = 1.5$ m *height in source and receiving room for direct and reverberation part of sound field.*

In contrast to the results presented in Figure 3 and Figure 4, where the sound source is place at the same position and just in different orientation, Figure 5 and Figure 6 show the effects of source orientation and position. The energy for all transmission paths is added and compared. Here we can conclude that in this case the diffuse part of the sound field smoothens the distribution of the SPL, so that the difference between average SPL on the partition between both cases is just 0.5dB.

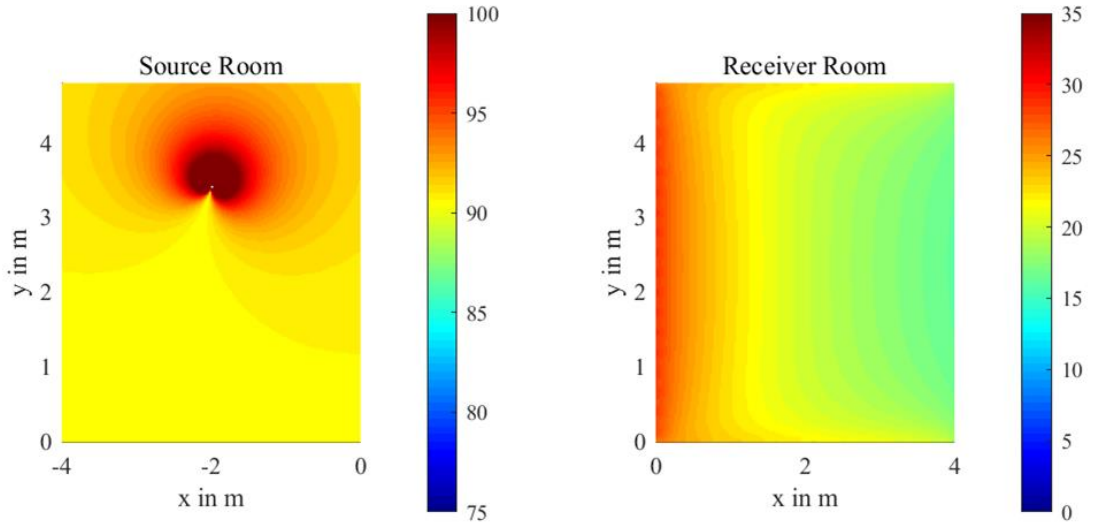

Figure 6: *Sound pressure level at* $z = 1.5$ m *height in source and receiver room for direct and reverb part of sound field.*

6.3 Verification of the standardized level difference (D_{nT})

The validation of proposed method in compliance with the ISO 12354 prediction model is shown by computing the D_{nT} from the simulated sound pressure values obtained for five different source and receiver positions, and by determining the reverberation time of receiving room (according to ISO 140). In Figure 7, the computed D_{nT} are shown for five random source positions and five random receiver positions. The mean value of the "simulated measurement" of D_{nT} obtained from

this approach agrees well with the input data of D_{nT}. Moreover, the D_{nT} values for the walls when considered as point sources are also computed and compared.

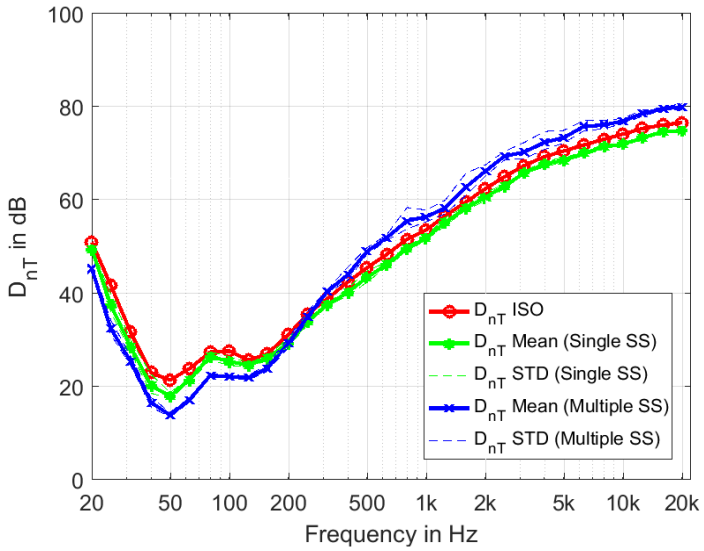

Figure 7: *Level difference between source and receiver room for all paths*

7. CONCLUSIONS

In this paper, we introduced an extended approach for auralization of sound insulation taking into account the source as well as receiving room acoustics and more detailed source information. The results of spatial variation of sound pressure on the building elements are presented using the knowledge of sound propagation theory in closed spaces. Room impulse responses for source and receiver rooms are synthesized from one-third octave band values to incorporate the reverberation effects in accordance with the absorption and geometries of the rooms. Therefore, this approach enables us to experience more realistic loudness, coloration and binaural impression of the sound transmission at the receiver by updating the sound source directivities and source and receiver positions in real-time. In addition, considering building elements as many secondary sources may help to include a more realistic directional cue of sound incidences. The results of real-time performance of algorithm in terms of latencies make it possible to render the sound insulation by taking into account the reasonable number of multiple point sources. Furthermore, in our ongoing research it is intended to address the challenges of bending wave patterns on the surfaces of walls and take into consideration outdoor moving sources in order to represent a complete building acoustics auralization framework integrated with virtual reality using audio-visual technology. The final goal is to provide a systems for psychoacoustic assessment of the impact of noise in buildings on humans in an ecologically valid manner.

8. ACKNOWLEDGEMENTS

This work is funded by HEAD-Genuit Foundation under Project ID: <P-17/4-W>.

9. REFERENCES

1. Vorländer, M, Schröder, D., Pelzer, S., Wefers, F., Virtual reality for architectural acoustics. Journal of Building Performance Simulation 8 (1), 2014, 15-25, DOI: 10.1080/19401493.2014.888594
2. Thaden, R., *Auralisation in Building Acoustics.* PhD Dissertation, Institute of Technical Acoustics, RWTH Aachen, Germany, 2007.

3. Imran, M., Heimes A., and M. Vorländer, *Auralization of Airborne Sound Transmission for Coupled Rooms in Virtual Reality*. Proc. DAGA Munich, 2018.
4. Imran, M., Heimes A., and Vorländer, M., *Auralization of Airborne Sound Transmission and Framework for Sound Insulation Filter Rendering*. Proc. Euronoise Crete 2018, 283-288.
5. Vorländer, M. and Imran, M., *Real-Time Auralization of Sound Insulation.* Proc. Internoise Crete 2018, 283-288.
6. Vorländer, M. and R. Thaden, *Auralisation of airborne sound insulation in buildings.* Acta Acustica united with Acustica **86**(1), 2000, 70-76.
7. ISO-12354-1, *Building acoustics: estimation of acoustic performance of buildings from the performance of elements–part 1: airborne sound insulation between rooms*. 2017
8. Kuttruff, H., *Room Acoustics*. CRC Press 2016
9. Rodriguez-Morales, A. *Real-time sound processing for interactive auralisation of sound insulation*. Proc. Forum Acusticum 2011, Aalborg, Denmark.